In vitro investigation of cellular effects of magnesium and magnesium-calcium alloy corrosion products on skeletal muscle regeneration

Title: *In vitro* investigation of cellular effects of magnesium and magnesium-calcium alloy corrosion products on skeletal muscle regeneration

Authors: Diana Maradze, Andrew Capel, Neil Martin, Mark P. Lewis, Yufeng Zheng, Yang Liu

PII: S1005-0302(19)30216-6
DOI: https://doi.org/10.1016/j.jmst.2019.01.020
Reference: JMST 1630

To appear in:

Received date: 28 November 2018
Revised date: 10 January 2019
Accepted date: 11 January 2019

Please cite this article as: Maradze D, Capel A, Martin N, Lewis MP, Zheng Y, Liu Y, *In vitro* investigation of cellular effects of magnesium and magnesium-calcium alloy corrosion products on skeletal muscle regeneration, *Journal of Materials Science and Technology* (2019), https://doi.org/10.1016/j.jmst.2019.01.020

In vitro investigation of cellular effects of magnesium and magnesium-calcium alloy corrosion products on skeletal muscle regeneration

Diana Maradze[1], Andrew Capel[2], Neil Martin[2], Mark P. Lewis[2], Yufeng Zheng[3], Yang Liu[1*]

[1] *Wolfson School of Mechanical, Electrical and Manufacturing Engineering, Loughborough University, Loughborough, Leicestershire, LE11 3TU, UK.*

[2] *School of Sport, Exercise and Health Sciences, Loughborough University, Loughborough, Leicestershire, LE11 3TU, UK.*

[3] *Department of Materials Science and Engineering, College of Engineering, Peking University, Beijing 100871, China.*

[Received 28 November 2018; revised 10 January 2019; accepted 11 January 2019]

*Corresponding author: *E-mail address*: Y.liu3@lboro.ac.uk (Yang Liu).

Biodegradable magnesium (Mg) has garnered attention for its use in orthopaedic implants due to mechanical properties that closely match to those of bone. Studies have been undertaken to understand the corrosion behaviour of these materials and their effects on bone forming cells. However, there is lack of research on how the corrosion of these biomaterials affect surrounding tissues such as skeletal muscle. Mg plays an important role in the structural and functional properties of skeletal muscle. It is therefore important to investigate the response of skeletal muscle cells to both soluble (Mg ions) and insoluble (corrosion granules) corrosion products. Through *in vitro* studies it is possible to observe the effects of corrosion products on myotube formation by the fusion of single muscle precursor cells known as myoblasts. To achieve this goal, it is important to determine if these corrosion products are toxic to myotubes. Here it was noted that although there was a slight decrement in cellular viability after initial exposure, this soon recovered to control levels. A high Ca/Mg ratio resulted in the formation of large myotubes and a low Ca/Mg ratio negatively affected myotube maturation. Mg^{2+} and Ca^{2+} ions are important in the process of myogenesis, and the concentration of these ions and the ratio of the ions to each other played a significant role in myotube cellular activity. The outcomes of this study could pave the way to a bio-informed and integrated approach to the design and engineering of Mg-based orthopaedic implants.

Keywords: Magnesium alloy, Corrosion, Biocompatibility, Muscle, Cellular Response, In Vitro

1. Introduction

Muscle, bone and tendon are integral components of the musculoskeletal system, and collectively these tissues work together to provide the framework of the body and determine movement and degree of flexibility. Damage to skeletal muscles can be caused by trauma, contusions and strains during sporting activities and these injuries can also result in bone fractures. The severity of the surrounding soft tissue damage and type of fracture influence the method of treatment. Furthermore, soft tissue injuries can cause significant clinical complications such as infection, soft tissue loss or non-union. Increase in delayed union and non-union have been reported when there is damage to skeletal muscle[1, 2]. During fracture healing, the lack of intact muscle has been shown to affect the healing process resulting in delayed bone deposition, callus remodelling, and reduced vascularisation[3]. It has also been shown that loss of large amounts of muscle tissue impairs fracture healing, whilst molecules released from intact muscle enhanced bone healing[4].

Complex fractures require fixation to hold the broken bones in the proper position for healing, with implants such as screws, plates, wires and nails being routinely used to reposition the bone fragments. The implants in current use for bone fixation are made from metals such as stainless steel and titanium, however the use of novel biodegradable Mg as orthopaedic implants has attracted attention as they have mechanical properties similar to bone[5–8]. Furthermore, studies have been published showing the successful use of Mg-based implants in clinical trials[9–11]. While there is considerable research on the influence of Mg alloy corrosion behaviour on bone forming cells, there is limited research on the effect on skeletal muscle cells.

When considering the responses of adult skeletal muscle to Mg ions, it is important to take into account its cellular physiology. Skeletal muscle fibres are terminally differentiated multinucleated cells, which shows great plasticity, and can undergo growth and atrophy in responses to a variety of stimuli through changes in gene expression. Muscle Ring Finger-1 (MuRF-1) and Muscle Atrophy F-box (MAFbx) are two such genes which are highly induced

in a variety of states of muscle atrophy[12,13] and are often used as markers of the early stages of muscle catabolism. In addition, skeletal muscle has the ability to regenerate due to a population of stem cells located between the sarcolemma and the basement membrane of terminally differentiated muscle fibres termed satellite cells. Following activation, satellite cells undergo asymmetric division to generate new satellite cells and myoblasts. The myoblasts proliferate to generate new myonuclei, and fuse together to form either new fibres or add to existing muscle fibres. As such, Mg ions have potential to impact skeletal muscle via post-natal or regenerative pathways. Mg also plays an important role in muscle function; and it has been shown that Mg deficiency can inhibit muscular growth[14] and negatively affect structural and functional properties of skeletal muscle[15]. The study presented here aims to investigate the responses of skeletal muscle cells to both soluble (Mg ions) and insoluble (corrosion granule) corrosion products of Mg and magnesium-calcium (Mg-Ca) alloy to test whether these products have any negative effects on skeletal muscle cell physiology.

2. Materials and methods

2.1. Mg Sample Preparation

Commercial pure Mg (99.9%) and Mg-Ca (1% Ca weight percentage) alloy in the form of cylindrical ingots were supplied by a partner from Peking University, Beijing, China[16]. Disks were machined from ingots and sterilised as previously described[17]]. Mg disks had average measurements of 12.2 mm (in diameter), 4.75 mm (in depth), and 1.00 g. Mg-Ca disks had average measurements of 16.0 mm (in diameter), 3.50 mm (in depth), and 1.50g.

2.2. Preparation of Mg corrosion products in vitro

Mg/Mg-Ca corrosion products were prepared as previously described[17]. Briefly Mg/Mg-Ca disks were immersed in 400mL of HyClone™ High Glucose Dulbecco's Modified Eagles Medium (Fisher Scientific, UK, DMEM) with L-glutamine (GE Healthcare, UK) and kept in a humidified atmosphere at 37°C and 5% CO_2 for 72 h. Part of the conditioned medium was filtered using a 0.22 μm sterile filter (Millipore, UK) to prepare a condition medium free of particulate (filtered medium), while the other half was left unfiltered (non-filtered medium). The stock conditioned medium (100) was diluted 1:2 (50),

1:4 (25) and 1:10 (10) with fresh DMEM and then supplemented with 7% (v/v) foetal bovine serum (FBS, Pan Biotech, UK) and 1% penicillin-streptomycin (Pen-Strep, Fisher).

2.3. Chemical Quantification of Major Ions in Corrosion Products

Following corrosion, the concentration of Mg^{2+} and Ca^{2+} ions in the conditioned media was analysed using inductively coupled plasma optical emission spectrometry (ICP-OES), (iCAP 6000 series, ThermoFisher Scientific, USA) and ITEVA analyst software (iCAP, ThermoFisher). Mg/Mg-Ca conditioned media were diluted and ICP-OES analysis was conducted as follows: 0.20 g, of the different concentrations of Mg/Mg-Ca filtered conditioned media was weighed and transferred into a tube, along with 0.40g of 2% v/v nitric acid and 9.50 g of deionized water. Calibration standards required for the construction of a standard curve covering the range of analyte concentration were prepared as follows: 28 element standards (100 ppm, Fisher) were serially diluted in 2% v/v nitric acid resulting in the following concentrations, 50 ppm, 5 ppm, 0.5 ppm and 0.05 ppm. 2% v/v nitric acid was used as blank controls and ICP-OES machine was used as per manufacturers' instructions. The measurement for Mg^{2+} and Ca^{2+} were measured at 279.5 and 317.9 wavelengths respectively. Each sample was measured in triplicate. Every time the conditioned medium was prepared and the ion concentration for Mg^{2+} and Ca^{2+} was measured.

2.4. Cell Culture

C2C12 murine skeletal muscle myoblast cell line (European Collection of Authenticated Cell Cultures, ECACC) was used for experimental procedures. Cells were cultured in a humidified environment at 37 °C and 5% CO_2 in growth medium (GM) comprised of 79 % DMEM (Fisher) supplemented with 20% (v/v) FBS (Pan Biotech) and 1% Pen-Strep (Fisher). Once the cells were confluent growth media was switched to differentiation medium (DM) comprising of 97% DMEM supplemented with 2% (v/v) horse serum (Life Technologies, UK) and 1% Pen-Strep. After 3 days of differentiation, the media was replaced with maintenance medium (MM) comprised of 92% DMEM supplemented with 7% (v/v) FBS and 1% Pen-Strep.

2.5. *Measurement of Cell Viability*

C2C12 were seeded onto 24 well plates at a density of 2×10^4 cells/well in triplicate. Cells were cultured in GM for 24 h. After 24 h C2C12 growth medium was switched to DM

for the fusion of myoblast into myotubes. After 3 days in DM, mature myotubes formed were further cultured in Mg/Mg-Ca filtered or non-filtered medium. Cells cultured in MM were used as the standard control. Viability of cells cultured with conditioned medium was measured using the AlamarBlue® reagent (Invitrogen, Life Technologies) after a total of 3 days in culture. AlamarBlue® cellular viability reagent stock solution was prepared by diluting 1:10 with unsupplemented DMEM. Cells were washed twice with 2 mL phosphate buffered saline (PBS) prior to being treated with 2 mL per well AlamarBlue® stock solution and humidified at 5 % CO_2 at 37 °C for 4 h. 100 µL per well of solution was then added to a black 96-well plate and analysed for fluorescence intensity. Increased fluorescence of AlamarBlue® reagent is indicative of an increase in cellular viability. Fluorescence level of the supernatant was measured at excitation: emission 530:590 nm and growth medium without cells was used as the blank sample. Fluorescence level from the background was subtracted from the fluorescence level of the treated and the control sample. Cell viability ≥ 70% relative to the control was defined as a non-toxic effect; this is in accordance to the ISO standard for biological evaluation of medical devices (ISO 10993-5:2009).

2.6. Myogenic genes expressed by C2C12 myoblasts

Mature myotubes formed as described earlier were treated with Mg/Mg-Ca conditioned media. RNA was extracted after 3 days of culture in Mg/Mg-Ca conditioned media using RNeasy Kit (QIAGEN, UK) as per manufacturers' instructions. The quantity and purity of RNA was measured using a Nanodrop spectrophotometer (ThermoFisher). The RNA produced was used for quantitative real time PCR (qRT-PCR) to amplify the primers of muscle related genes: MAFbx and MuRF1 using a one-step real time PCR machine (ViiA 7, Applied Biosystems), QuantiFast SYBR Green RT-PCR Kit (QIAGEN, UK) and reverse and forward primers designed and validated within house (Table.1). RP2-β was used as the endogenous control. Amplification was performed for 40 cycles, consisting of reverse transcription at 50 °C for 10 min, DNA polymerase activation at 95 °C for 5 min, denaturation at 95 °C for 10 s and annealing/extension at 60 °C for 30 seconds. Melting curves were generated to distinguish and exclude non-specific amplifications and primer dimers. Ct values were analysed by the comparative Ct (ΔΔCt) method. Ct value of each sample was normalised with the average Ct value of the endogenous control. The fold change in gene expression was calculated as $2(^{-\Delta\Delta Ct})$.

2.7.Mature myotube actin filament staining

Glass cover slips were pre-coated with 1 mL of 0.2% gelatin solution (Sigma Aldrich, UK) and incubated for 30 minutes to allow attachment of cells to the surface. Cells were seeded on the cover slips in a six well plate at a seeding density of 1×10^5 cells/well. Cells were cultured in GM until confluent. Once the cells were confluent medium was switched to DM for the fusion of myoblast into myotubes. After 3 days in DM mature myotubes were formed, and the medium was changed to Mg/Mg-Ca filtered and non-filtered medium. After 3 days culture in Mg/Mg-Ca conditioned media cells were fixed with 2% formaldehyde (Sigma) for 30 min. Fixed cells were stained with rhodamine phalloidin (1:40, Life Technologies) and 4',6-diamidino-2-phenylindole (DAPI, 1:1000, Sigma). The cells were left for 60 min at room temperature in the dark. After incubation the fixed cells on cover slips were mounted on glass slides for imaging. The cells were visualised with a Leica DM2500 fluorescence microscope to determine degree of differentiation.

2.8. Image analysis of myotubes

A multinucleated myotube is formed when myoblasts fuse together. The number of nuclei per myotube can be used as an indication of myotube size. The more myoblasts that fuse together the bigger the myotube and the higher the number of nuclei present per myotube. For analytical purposes, a myotube was defined as a cell unit that stained positive for phalloidin and containing at least 3 nuclei. 21 images from 3 biological repeats for each sample treated with various concentrations of Mg/Mg-Ca conditioned media were analysed. For myotubes treated with Mg/Mg-Ca conditioned media, size of myotubes were organized into 4 groups, 3-10 nuclei/myotube (small), 11-50 nuclei/myotube (medium), 51-100 nuclei/myotube (large) and 101-300 nuclei/myotube (extra-large). Average myotube width was also quantified for each of these conditions.

2.9. Statistical analysis

Statistical analysis was performed using SPSS software (IBM, USA), multivariate analysis of variance and one-way ANOVA, including Tukey's post hoc tests, were performed to detect significant ($p < 0.05$) effects of the experimental variables.

3. Results

3.1. Chemical analysis of corrosion products in the conditioned media

ICP-OES was used to measure the amount of Mg^{2+} and Ca^{2+} ions present in the conditioned medium following the corrosion of Mg/Mg-Ca biomaterials *in vitro*. As indicated in Table 2, the concentration of Ca^{2+} ions in Mg100 conditioned media was reduced to 0.8mM, significantly less than was present in the control (2.2 mM). But as the conditioned media was diluted to Mg50, Mg25 and Mg10 the concentration of Ca^{2+} ions was replenished by the addition of fresh medium and the Ca/Mg ratio was also increased. The dilution of the conditioned media also resulted in the reduced concentration of Mg^{2+} ions. Mg-Ca alloy corroded slower than pure Mg leading to less Mg^{2+} ions being released into the medium as indicated in Table 3. The highest concentration of Mg^{2+} ions detected in Mg-Ca100 conditioned medium (3.9 mM) was 4 times less than the concentration detected in Mg100 conditioned medium (16.9 mM). As observed with pure Mg corrosion, the corrosion of Mg-Ca also resulted in the depletion of Ca^{2+} ions from the medium, however the Ca/Mg ratio of Mg100 conditioned medium was 10 times less compared to Mg-Ca100 conditioned medium.

3.2.Responses of myotubes to the presence of conditioned media

A reduction in metabolic activity was observed when cells were cultured in Mg filtered medium on day 1, however metabolic activity was improved by days 2 and 3. In non-filtered medium, low metabolism was only observed in samples treated with Mg25 and Mg10 at day 1. Overall the metabolic activity of Mg treated myotubes was still above 70% throughout the culture period, even at the highest concentration of 16.9 mM (Mg100), suggesting no cytotoxic effects for both filtered and non-filtered medium (Fig. 1).

The treatment of myotubes in the presence of Mg-Ca conditioned media (filtered and non-filtered medium) resulted in an increase in metabolic activity when comparing the various concentrations to the control at each time point (Fig.2), with a maximum increase of 1.5 times observed in MgCa100 filtered media at day 2 of culture. However, by day 3 a reduction in metabolic activity was observed compared to days 1 and 2 across conditions, particularly in non-filtered medium, but activity was still above the control.

3.3. Morphological analysis of myotubes following treatment with conditioned media

Fig. 3 shows images of myotubes captured on day 3 of culture in Mg conditioned media. The morphological observations demonstrated a slight reduction in total nuclei number per

image across all conditions when compared to control, however these differences were not significant indicating that a healthy cellular population was present across each of the conditions (Fig. 4(A)). Average myotube widths were comparable to control in each of the culture conditions, with the exception of Mg50 non-filtered medium which demonstrated increased widths compared to both control and each of the filtered media conditions ($p < 0.01$). However, a general trend was observed indicating increased myotube widths in the cells cultured in all the Mg non-filtered conditions, when compared to both control and the Mg filtered conditions (Fig. 4(B)).

Imaging analysis was also performed to quantify the size distribution of myotubes presented in the field of view of randomly selected images based on the number of nuclei contained. When cells were treated with Mg100 conditioned media (filtered and non-filtered medium) there was a significantly higher ($p < 0.001$) percentage (80%) of small myotubes compared to the control (50%) (Fig. 5(A)). However, when the concentration of Mg conditioned media (filtered and non-filtered medium) was diluted to Mg50 this effect on myotube size was reduced by at least 20%. Further dilution resulted in myotube size distribution similar to the control. However, treatment with Mg10 non-filtered medium resulted in a significantly lower ($p < 0.05$) percentage of smaller myotubes and a significantly higher ($p < 0.05$) percentage of medium sized myotubes in comparison to Mg100 non-filtered medium (Fig. 5(B)). The average number of myotubes per image increased significantly in the filtered Mg100 and Mg50 conditions compared to the non-filtered Mg50 and Mg25 conditions ($p < 0.05$) (Fig. 5(C)). Overall, the addition of non-filtered Mg appeared to promote increases in myotube size, which was offset by a reduction in the number of myotubes present per field of view.

Fig. 6 shows images of myotubes captured on day 3 of culture in MgCa conditioned media. Myotubes cultured within both filtered and non-filtered MgCa conditions demonstrated a non-significant reduction in total nuclei number per image across all conditions when compared to control (Fig. 7(A)). Average myotube widths were significantly increased in both MgCa25 and MgCa10 filtered media ($p < 0.05$), as well as MgCa25 and MgCa10 non-filtered media ($p < 0.01$) conditions when compared to control. Significant increases in width were also observed between the MgCa25 and MgCa10 non-filtered media, and MgCa100 and MgCa50 filtered media conditions ($p < 0.01$ in both cases) (Fig. 7(B)).

Myotube size, expressed as total nuclei per myotube, was increased in MgCa100 filtered medium (Fig. 8(A)); there was a significantly higher percentage ($p < 0.05$) of smaller myotubes compared to MgCa10 filtered medium. Furthermore, treatment of myotubes with MgCa25 and MgCa10 filtered medium resulted in a higher percentage ($p < 0.01$) of extra-large myotubes compared to the control. When cells were cultured in Mg-Ca non-filtered media (Fig. 8(B)), myotube size distribution was similar to the control for all the concentrations. Finally, number of myotubes per field of view were significantly lower in the filtered MgCa25 and MgCa10 condition, when compared with the non-filtered MgCa100 condition ($p < 0.05$) (Fig. 8(C)). Overall when myotubes were cultured in filtered medium at lower concentrations there was an increase in myotube size, which was again largely offset by a corresponding reduction in the number of myotubes present per field of view.

3.4. Effect of Mg and Mg-Ca conditioned media on myotubes at gene level

Gene analysis was performed to investigate the effects of high concentrations of Mg corrosion products on myotubes. The expression of MurF1 and MAFbx was investigated following treatment with Mg conditioned media. Gene analysis was performed on cells treated with Mg concentration ≥ 10mM (Mg100 and Mg50). The treatment of myotubes with Mg filtered and non-filtered medium downregulated (*, $p < 0.05$) MurF1 expression compared to the control (Fig. 9(A)), whereas the expression of MAFbx was upregulated when myotubes were treated with Mg100 non-filtered medium compared to control; however, only 0.4 fold changes was observed (Fig. 9(B)). The observed 0.4 fold changes is not a significant indicator of muscle atrophy, therefore it can be concluded that the presence of Mg conditioned medium does not cause atrophy related damage to the mature myotubes.

4. Discussion

The corrosion of Mg/Mg-Ca alloy resulted in the release of Mg^{2+}, Ca^{2+} and phosphates ions into the medium[17, 18]. Corrosion of Mg/Mg-Ca alloy also led to an increase in pH of the culture media[19]. However, the presence of sodium carbonate in DMEM and exposure to CO_2 during cell culture resulted in the formation of a CO_2/bicarbonate buffering system, similar to that in blood[20] , and the formation of the corrosion layers and the kinetics of corrosion processes further affects the of Mg2+ release profile as illustrated in our previous numerical study[21]. The degradation behaviour of the two metals, pure Mg and Mg-Ca alloy resulted in two different media environments. The differences in these environments had an

impact on the muscle culture. The initial exposure of Mg conditioned medium to myotubes resulted in a decrease in metabolic activity; however metabolic activity was still above 70% when compared to the control for all concentrations at all time points, suggesting no cytotoxic effects. In the presence of Mg conditioned medium, muscle cells were exposed to a higher Mg^{2+} concentration and the Ca/Mg ratio was negatively correlated with Mg^{2+} concentration when the conditioned medium was diluted. It was noted that the Ca/Mg ratio in the control was 20 times higher than in Mg100 and Mg50. On the other hand, when muscle cells were exposed to Mg-Ca conditioned medium the opposite effect was observed. Metabolic activity of myotubes was significantly enhanced compared to the control, suggesting that Mg^{2+} ion concentration of 4mM or less and higher Ca/Mg ratio is beneficial for myotube cellular activities. Rubin et al., showed that Ca^{2+} ion deprivation inhibited DNA synthesis, however high Mg^{2+} ion concentration reversed the effects of low Ca^{2+} ion concentration[22]. Hence, the variation of metabolic activity of myotubes in Mg conditioned medium could be attributed to cellular responses to high Mg^{2+} ion concentration, which counteracted the Ca^{2+} ion deficiency effect.

Overall, the presence of Mg filtered media appeared to have negligible overall effect on the size of myotubes, whereas the presence of Mg non-filtered appeared to promote increases in myotube size, which was offset by a reduction in the number of myotubes present per area. However, it was also noted that the treatment of myotubes with high Mg^{2+} ion concentration (Mg100 filtered and non-filtered media) resulted in a reduction in the number of nuclei contained per myotube, an indication of muscle size/fusion. When myoblast cells are induced to differentiate, not all myoblast cells form myotubes; a mixed population of myoblasts and mature myotubes exist. Most likely in the presence of high Mg^{2+} ion concentration (Mg100), mature myotubes detached from the culture substrate. On the other hand, the unfused myoblasts where able to initiate fusion; but due to low Ca^{2+} ion concentrations (below 1.5mM), the fusion process was ineffective resulting in the formation of smaller myotubes (low nuclei number/myotube). Ca^{2+} ion concentrations of 1.5mM are required for proper fusion of myoblasts[23]. Furthermore, the low Ca^{2+} ion concentration in Mg100 could have compromised the capability of fused myotubes to maintain the cytosolic calcium level required via store-operated entry mechanisms[24]. Even though Mg^{2+} ions have been reported to play a role in fusion, Ca^{2+} ions are the key player as high concentrations (10 mM) of Mg^{2+} ions are required to compensate for Ca^{2+} ion deficiency[25]. Important proteins required for fusion such as calpains and integrins [26, 27] are Ca^{2+} ion dependent. Improper function of these

proteins affects myotube formation resulting in short myotubes and accumulation of unfused cells[28].

The effect of high Mg conditioned medium concentration was also analysed at the gene level. Gene expression analysis of MAFbx and MuRF1 did not show atrophy related effects; in fact a down regulation of these atrophy related genes was observed. Furthermore, implantation of Mg *in vivo* did not show muscle damage[28], hence it can be concluded that Mg and its corrosion products do not cause adverse effects on skeletal muscle. It has been identified that cellular response to extracellular Mg^{2+} ion concentration depends on cell type and the differentiation stage of the treated cells[29]. The reduced size of myotubes observed may imply that the high concentration of Mg conditioned media could also play a role in metabolic activities during myoblast differentiation and tissue maturation[30].

On the other hand, exposure to Mg-Ca conditioned media resulted in large or hypertrophic myotubes. Fusion of myoblasts to myotubes or myotubes to myotubes indicates a high rate of protein synthesis[28]. The increase in metabolic activity observed here and also proved by the previously published proteomic data could have contributed to the formation of large myotubes[31]. It is believed that maintaining a high Ca/Mg ratio is important in the formation of large myotubes; calcium dependent signalling has been shown to be involved in the induction of hypertrophy[32]. It can be concluded that a high Mg^{2+} ion concentration is required for accelerating cell proliferation but the availability of Ca^{2+} ions is crucial for myotube formation.

This is the first and only study to date to demonstrate the effect of Mg and Mg-Ca corrosion products on mature myotubes *in vitro*. This study has revealed the importance of not only looking at bone forming cells but also muscle cells when investigating bone regeneration in the presence of a corroding Mg implant. Future research on Mg biomaterial engineering should also consider the interaction of alloyed element released during corrosion process, with the corresponding biological system that the biomaterials are intended to be used.

5. Conclusions

Concentration of Mg^{2+} ions and the ratio between Mg^{2+} and Ca^{2+} ions play a significant role in maintaining the cellular activities of myoblasts and muscle regeneration. Initial exposure of myotubes to high Mg corrosion product concentration reduced cell viability, but

over time the myotubes were able to adapt. Over the time period investigated, cells responded differently to Mg and Mg-Ca conditioned media. A high Ca/Mg ratio resulted in the formation of large myotubes and a low Ca/Mg ratio resulted in small sized myotubes. High Mg^{2+} ion concentration between 4-10mM can accelerate cell proliferation but the availability of Ca^{2+} ion is crucial for myotube formation.

Acknowledgements

DM's PhD studentship was supported by The EPSRC (EP/F500491/1) Centre of Doctor Training in Regenerative Medicine and SkelGen under Marie Skłodowska-Curie Research and Innovation Staff Exchange programme (FP7-PEOPLE-2012-IRSES, 318553).

References

[1] R. Abou-Khalil, F. Yang, S. Lieu, A. Julien, J. Perry, C. Pereira, F. Relaix, T. Miclau, R. Marcucio, C. Colnot, *Stem Cells* 33 (2015) 1501–11.

[2] M. K. Sen, T. Miclau, *Injury* 38 (SUPPL. 1) (2007) 2007.

[3] R. Abou-Khalil, F. Yang, M. Mortreux, S. Lieu, Y. Y. Yu, M. Wurmser, C. Pereira, F. Relaix, T. Miclau, R. S. Marcucio, C. Colnot, *J. Bone Miner. Res.* 29 (2014) 304–315.

[4] C. Tagliaferri, Y. Wittrant, M. J. Davicco, S. Walrand, V. Coxam, *Ageing Res. Rev.* 21 (2015) 55–70.

[5] F. Witte, V. Kaese, H. Haferkamp, E. Switzer, A. Meyer-Lindenberg, C. J. Wirth, and H. Windhagen, *Biomaterials* 26 (2005) 3557–3563.

[6] F. Witte, N. Hort, C. Vogt, S. Cohen, K. U. Kainer, R. Willumeit, and F. Feyerabend, *Curr. Opin. Solid State Mater. Sci.* 12 (2008) 63–72.

[7] D. Hong, P. Saha, D. T. Chou, B. Lee, B. E. Collins, Z. Tan, Z. Dong, and P. N. Kumta, *Acta Biomater.* 9 (2013) 8534–8547.

[8] Y. Zhang, J. Xu, Y. C. Ruan, M. K. Yu, M. O'Laughlin, H. Wise, D. Chen, L. Tian, D. Shi, J. Wang, S. Chen, J. Q. Feng, D. H. K. Chow, X. Xie, L. Zheng, L. Huang, S. Huang, K. Leung, N. Lu, L. Zhao, H. Li, D. Zhao, X. Guo, K. Chan, F. Witte, H. C. Chan, Y. Zheng, and L. Qin, *Nat. Med.* 22 (2016) 1160–1169.

[9] D. Zhao, S. Huang, F. Lu, B. Wang, L. Yang, L. Qin, K. Yang, Y. Li, W. Li, W. Wang, S. Tian, X. Zhang, W. Gao, Z. Wang, Y. Zhang, X. Xie, J. Wang, and J. Li, *Biomaterials* 81 (2016) 84–92.

[10] J.W. Lee, H.S. Han, K.J. Han, J. Park, H. Jeon, M.R. Ok, H.K. Seok, J.P. Ahn, K.E. Lee, D.H. Lee, S.J. Yang, S.Y. Cho, P.R. Cha, H. Kwon, T.H. Nam, J.H. Lo Han, H.J. Rho, K.S. Lee, Y.C. Kim, and D. Mantovani, *Proc. Natl. Acad. Sci. U. S. A.*, vol. 113, no. 3, pp. 716–721, Jan. 2016.

[11] H. Windhagen, K. Radtke, A. Weizbauer, J. Diekmann, Y. Noll, U. Kreimeyer, R. Schavan, C. Stukenborg-Colsman, and H. Waizy, *Biomed. Eng. Online* 12 (2013) 62.

[12] S. C. Bodine, E. Latres, S. Baumhueter, V. K. Lai, L. Nunez, B. A. Clarke, W. T. Poueymirou, F. J. Panaro, E. Na, K. Dharmarajan, Z. Q. Pan, D. M. Valenzuela, T. M. DeChiara, T. N. Stitt, G. D. Yancopoulos, and D. J. Glass, *Science* 294 (2001) 1704–1708.

[13] S. H. Lecker, R. T. Jagoe, A. Gilbert, M. Gomes, V. Baracos, J. Bailey, S. R. Price, W.

E. Mitch, and A. L. Goldberg, *FASEB J. Off. Publ. Fed. Am. Soc. Exp. Biol.* 18 (2004) 39–51.

[14] Y. Furutani, M. Funaba, and T. Matsui, *Cell Biochem. Funct.* 29 (2011) 577–581.

[15] C. Astier, E. Rock, C. Lab, E. Gueux, A. Mazur, and Y. Rayssiguier, *Free Radic. Biol. Med.* 20 (1996) 667–674.

[16] Z. Li, X. Gu, S. Lou, and Y. Zheng, *Biomaterials* 29 (2008) 1329–1344.

[17] D. Maradze, D. Musson, Y. Zheng, J. Cornish, M. Lewis, and Y. Liu, *Sci. Rep.* 8 (2018) 10003.

[18] R. Q. Hou, N. Scharnagl, F. Feyerabend, and R. Willumeit-Römer, *Corros. Sci.* 132 (2018) 35–45.

[19] R. Harrison, D. Maradze, S. Lyons, Y. Zheng, and Y. Liu, *Prog. Nat. Sci. Mater. Int.*, 24 (2014) 539–546.

[20] R. Willumeit, J. Fischer, F. Feyerabend, N. Hort, U. Bismayer, S. Heidrich, and B. Mihailova, *Acta Biomater.* 7 (2011) 2704–2715.

[21] S. K. Ahmed, J. P. Ward, Y. Liu, *Materials* 11 (2018) 1.

[22] A. H. Rubin, M. Terasaki, and H. Sanui, "Major intracellular cations and growth control: correspondence among magnesium content, protein synthesis, and the onset of DNA synthesis in BALB/c3T3 cells," *Proc. Natl. Acad. Sci. U. S. A.*, vol. 76, no. 8, pp. 3917–3921, Aug. 1979.

[23] B. B. Friday, V. Horsley, and G. K. Pavlath, *J. Cell Biol.* 149 (2000) 657–666.

[24] C.-H. Cho, J. S. Woo, C. F. Perez, and E. H. Lee, *Exp. Mol. Med*. vol. 49. The Author(s), p. e378, Sep-2017.

[25] D. Kirchhofer, J. Grzesiak, and M. D. Pierschbacher, *J. Biol. Chem.* 266 (1991) 4471–4477.

[26] B. Leitinger, A. McDowall, P. Stanley, and N. Hogg, *Biochim. Biophys. Acta* 1498 (2000) 91–98.

[27] V. Horsley and G. K. Pavlath, *Cells Tissues Organs* 176 (2004) 67–78.

[28] M. Schwander, M. Leu, M. Stumm, O. M. Dorchies, U. T. Ruegg, J. Schittny, and U. Muller, *Dev. Cell* 4 (2003) 673–685.

[29] S. Chen, L. Tan, B. Zhang, Y. Xia, K. Xu, and K. Yang, *J. Mater. Sci. Technol.* 33 (2017) 469–474.

[30] G. Farruggia, S. Castiglioni, A. Sargenti, C. Marraccini, A. Cazzaniga, L. Merolle, S. Iotti, C. Cappadone, and J. A. M. Maier, *Magnes. Res.* 27 (2014) 25–34.

[31] Z. Zhen, B. Luthringer, L. Yang, T. Xi, Y. Zheng, F. Feyerabend, R. Willumeit, C.

Lai, and Z. Ge, *Mater. Sci. Eng. C* 69 (2016) 522–531.

[32] S. E. Dunn, J. L. Burns, R. N. Michel, *J. Biol. Chem.* 274(199) 21908–21912.

Figure captions

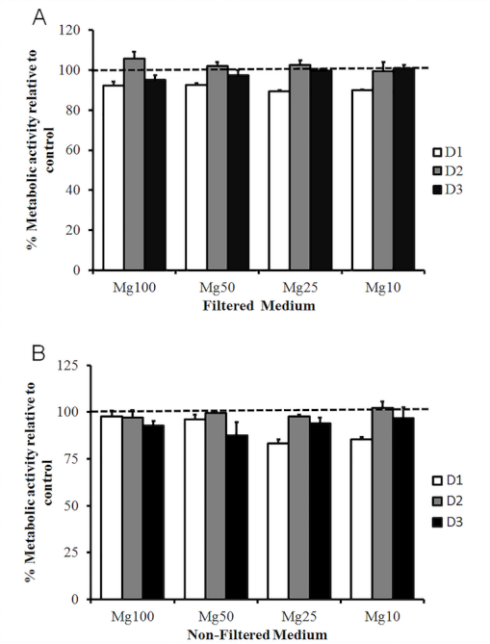

Fig.1. Effect of Mg conditioned media on mature myotube metabolic activity was investigated using the AlamarBlue® assay. Myotubes were cultured in various concentrations of (A) Mg filtered medium and (B) Mg non-filtered medium over a period of 3 days. Metabolic actvity for all concentrations at all time points was above 70%, suggesting no cytotoxic effects. The dotted line at 100% metabolic activity represents the control. The bars represent the mean and standard deviation in the positive orientation of three independent experiments, each with *n*=3.

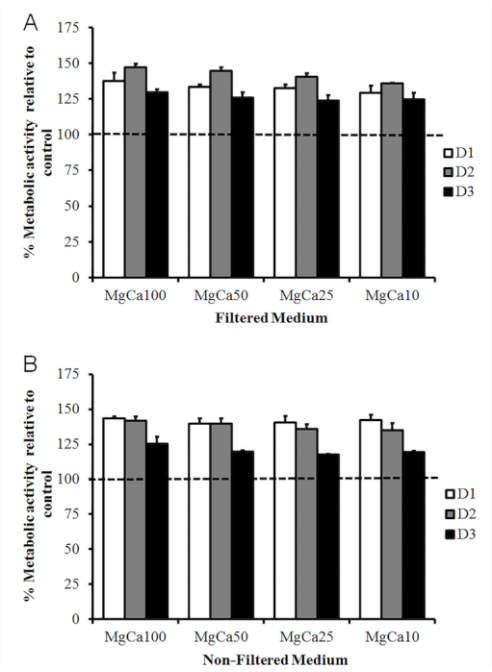

Fig.2. Effect of Mg-Ca conditioned media on mature myotube metabolic activity was investigated using the AlamarBlue® assay. Myotubes were cultured in various concentrations of (A) Mg-Ca filtered medium and (B) Mg-Ca non-filtered medium over a period of 3 days. Treatment with Mg-Ca conditioned media resulted in enhanced metabolic activity. The dotted line at 100% metabolic activity represents the control. The bars represent the mean and standard deviation in the positive orientation of three independent experiments, each with n=3.

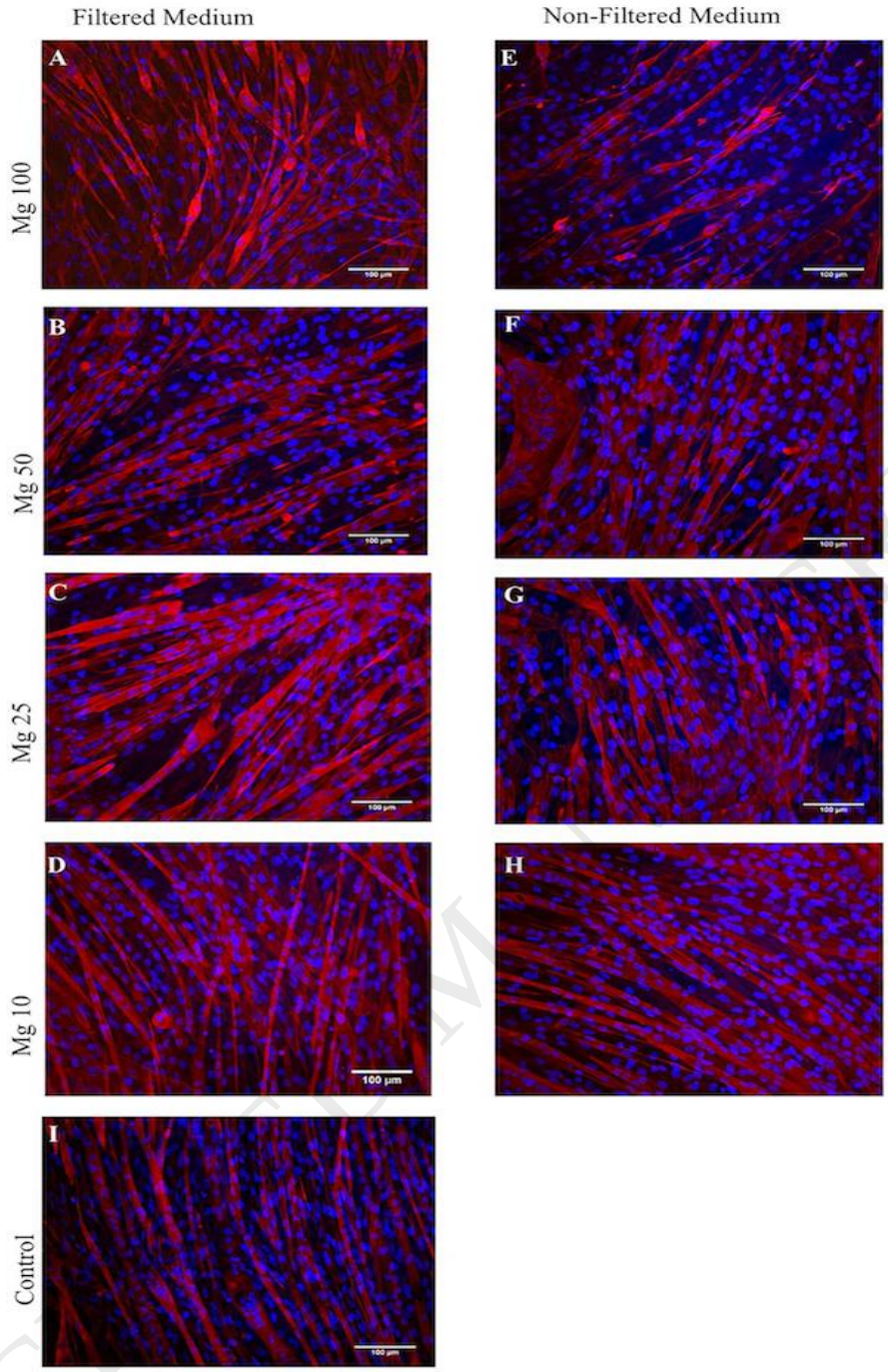

Fig.3. Representative images showing actin filament staining of myotubes after treatment with various concentrations of Mg conditioned media. (A-D) Images showing the effect of filtered medium on myotubes and (E-H) images showing the effect of non-filtered medium on myotubes. (I) Image showing cells cultured in the standard growth medium (control). Scale bar= 100µm.

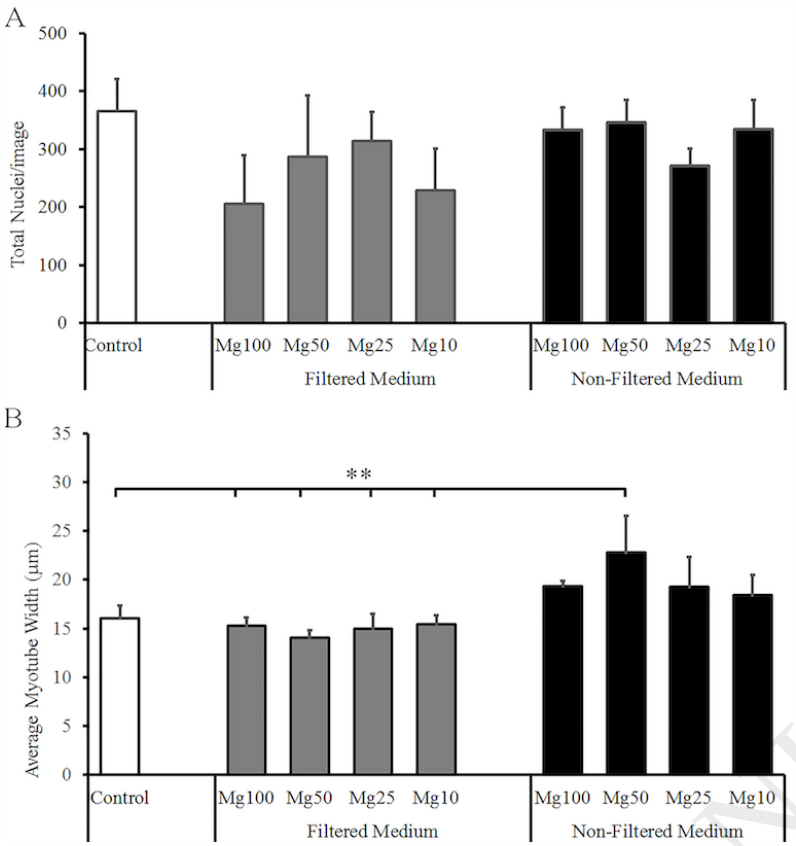

Fig.4. Myotube width analysis following treatment with Mg conditioned medium. (A). No significant differences in total nuclei number per image across all conditions were detected when myotubes were treated with Mg conditioned medium. (B) When myotubes were treated with Mg50 non-filtered medium an increase in myotube width was observed when compared to both control and each of the filtered media conditions (**, $p < 0.01$).

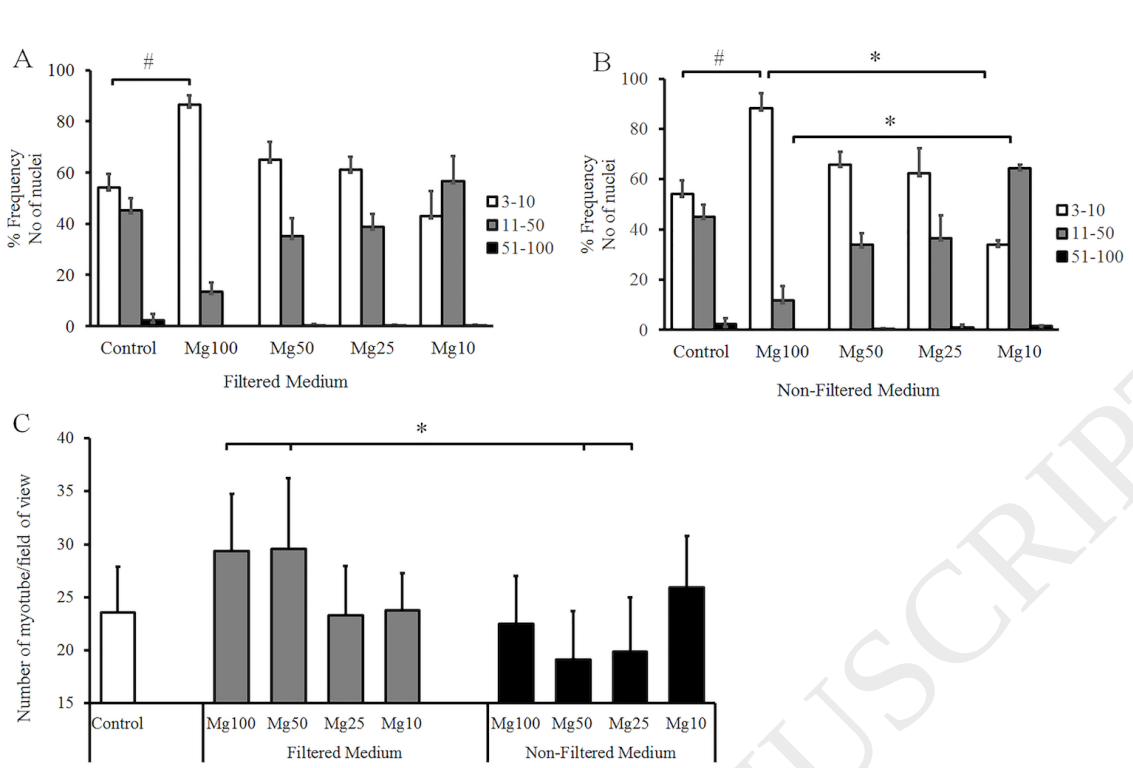

Fig.5. Image analysis of stained myotubes following treatment with Mg filtered and non-filtered medium. (A) Treatment with Mg100 filtered medium resulted in a significantly high (#, $p < 0.001$) percentage of smaller myotubes (3-10 nuclei/myotube) compared to control. (B) Treatment with Mg100 non-filtered medium also resulted in a significantly high (#, $p < 0.001$) percentage of smaller myotubes compared to control. (C) There was a significant increase (*, $p < 0.05$) in the number of myotubes per field of view when myotubes were treated with Mg100 and Mg50 filtered medium compared to treatment with Mg50 and Mg25 non-filtered medium. The bars represent the mean and standard deviation in the positive orientation of three independent experiments, each with n=3.

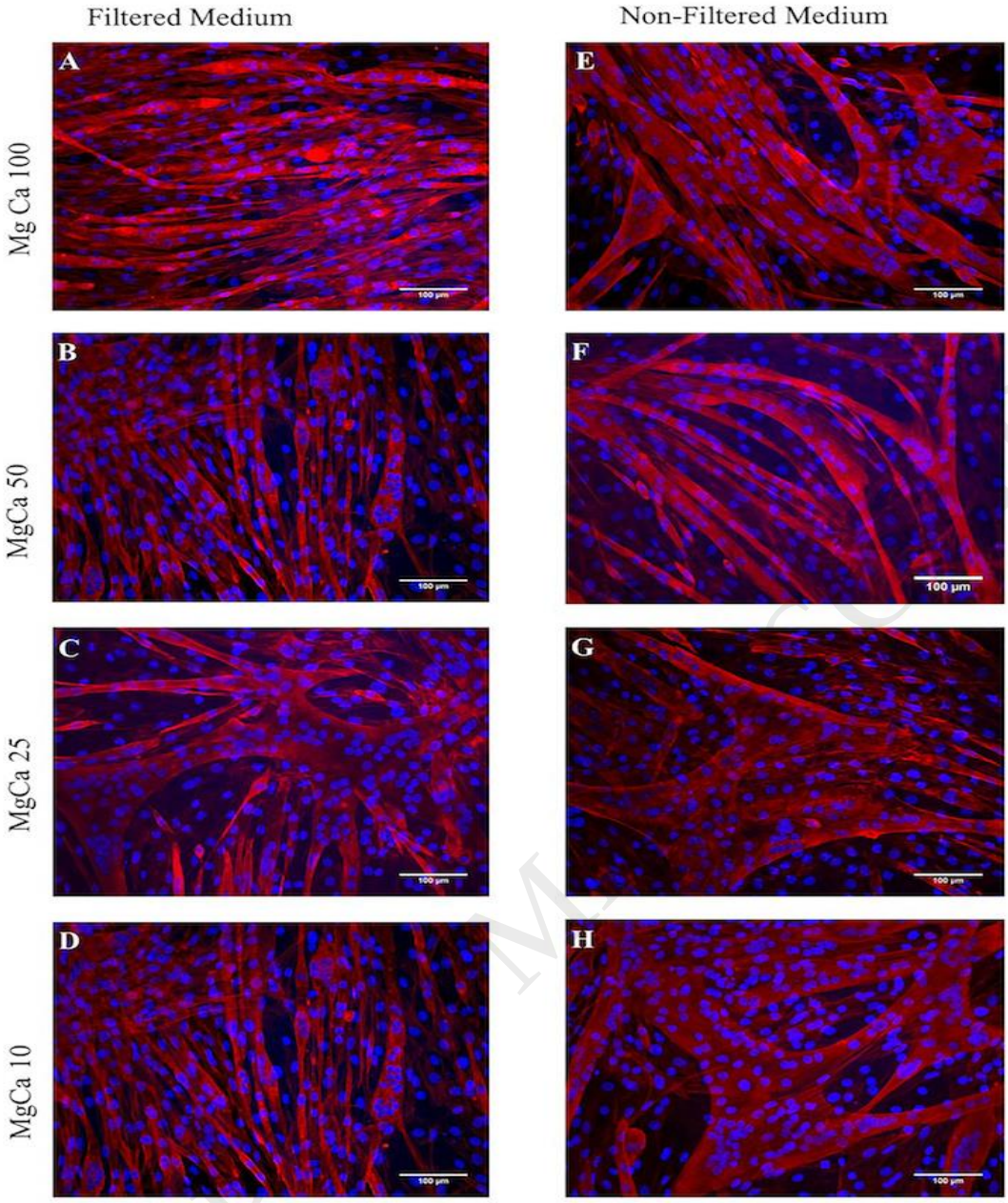

Fig.6. Representative images showing actin filament staining of myotubes after treatment with various concentrations of Mg-Ca conditioned media. (A-D) Images showing the effect of filtered medium on myotubes and (E-H) images showing the effect of non-filtered medium on myotubes. No adverse effects were seen when myotubes were treated with Mg-Ca conditioned medium; treatment with Mg-Ca resulted in the formation of larger myotubes compared to the control. Scale bar= 100µm.

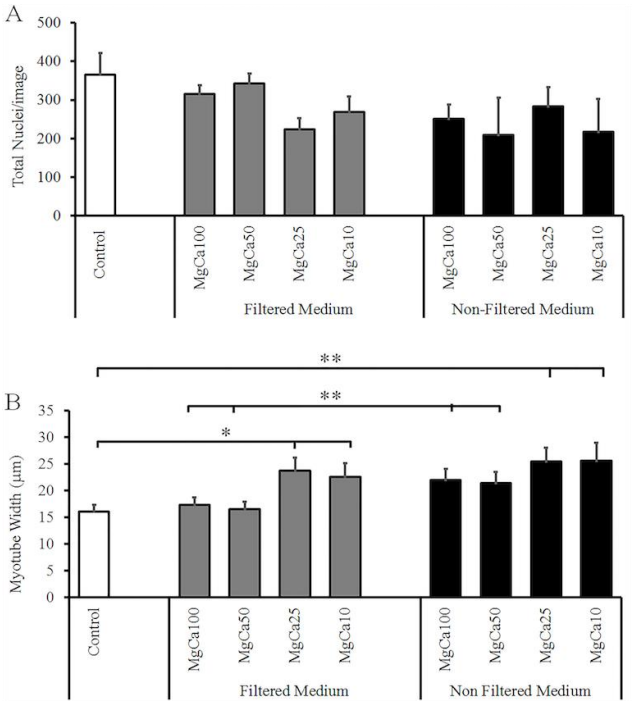

Fig.7. Myotube width analysis following treatment with MgCa conditioned medium. (A). Culture of myotubes in MgCa conditioned media demonstrated a non-significant reduction in total nuclei number per image across all conditions when compared to control. (B). A significant increase in average myotube widths was observed in both filtered MgCa25 and MgCa10 (*, $p < 0.05$), as well as non-filtered MgCa25 and MgCa10 (**, $p < 0.01$) conditions when compared to control. Significant increases in myotube width were also observed between MgCa25 and MgCa10 non-filtered media, and MgCa100 and MgCa50 filtered medium (**, $p < 0.01$).

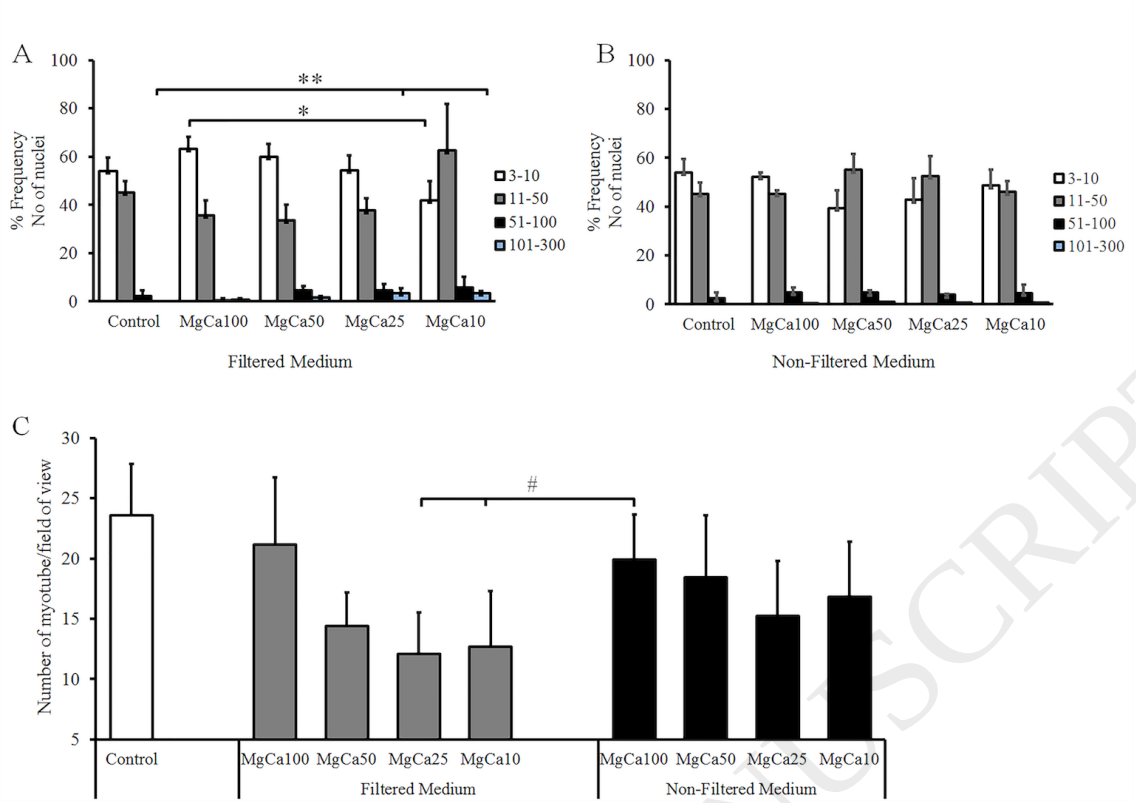

Fig.8. Image analysis of the stained myotubes following treatment with Mg-Ca conditioned media. (A) When myotubes were treated with filtered medium, myotube size distribution followed a trend similar to the control. However, treatment of myotubes with MgCa25 and MgCa10 filtered medium resulted in a higher percentage ($p < 0.01$) of extra-large myotubes compared to control. (B) The treatment of myotubes with Mg-Ca non-filtered medium also resulted in a size distribution similar to control. (C) Treatment of cells with MgCa25 and MgCa10 filtered medium resulted in a significantly lower (#, $p < 0.01$) myotube number as measured per field of view compared to treatment with MgCa100 non-filtered medium.

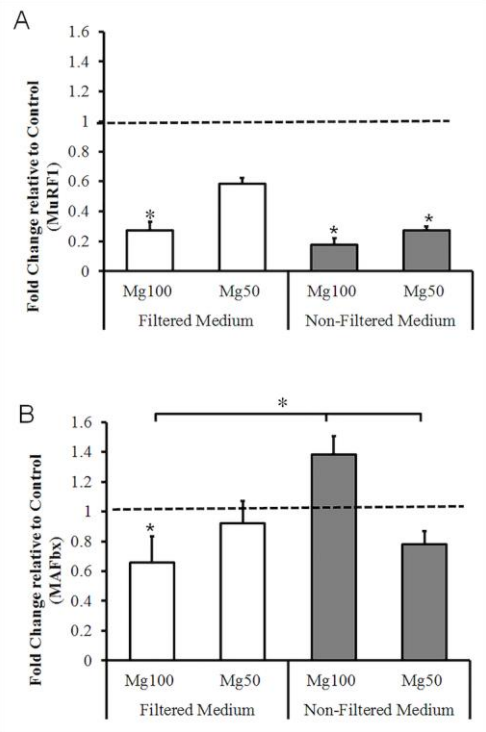

Fig.9. The effect of corrosion products at gene level on myotubes treated with Mg conditioned medium for 3 days. (A) Fold change in the gene expression of MuRF1 following treatment with Mg conditioned medium. Treatment of myotubes with Mg conditioned medium resulted in a significant downregulation (*, $p < 0.05$) of MurF1. (B) Treatment of myotubes with the presence of Mg100 non-filtered medium resulted in a significant increase (*, $p < 0.05$) in the expression of MAFbx compared to Mg100 filtered and Mg50 non-filtered medium. A significant downregulation of MAFbx was also observed when myotubes were treated with Mg100 filtered medium compared to control. The fold change is relative to the control sample, represented by a fold change of 1 (dotted line). Target gene expression was normalised to the endogenous control (RP2-β). The bars represent the mean and standard deviation in the positive orientation of two independent experiments, each with n=3.

Table 1: Sequence of the primers for muscle related genes

Species	**Gene of interest**	**Forward Primer (5'-3')**	**Reverse Primer (5'-3')**
Mouse	MuRF-1	CCA AGG AGA ATA GCC ACC AG	CGC TCT TCT TCT CGT CCA G
	MAFbx	CTG AAA GTT CTT GAA GAC CAG	GTG TGC ATA AGG ATG TGT AG
	RP2-β	GGT CAG AAG GGA ACT TGT GGT AT	GCA TCA TTA AAT GGA GTA GCG TC

Table 2: Concentration of Ca^{2+} and Mg^{2+} ions in the conditioned media following the corrosion of pure Mg

Ion concentration (mean ±SD)			
Sample	Ca (mM)	Mg (mM)	Ca:Mg
Mg100	0.8±0.2	16.9±1.1	0.05
Mg50	1.2±0.2	10.8±1.2	0.1
Mg25	1.5	4.9±0.4	0.3
Mg10	2.1±0.7	3.1±0.7	0.7
Control	2.2±0.6	0.9±0.2	2.0

Table.3: Concentration of Ca^{2+} and Mg^{2+} ions in the conditioned media following the corrosion of Mg-Ca

Ion concentration (mean ±SD)			
Sample	Ca (mM)	Mg (mM)	Ca:Mg
MgCa100	1.9±0.3	3.9±1.1	0.5
MgCa50	1.7±0.1	2.4±1.2	0.7
MgCa25	1.7±0.3	1.6±0.4	1.0
MgCa10	2.2±0.4	1.2±0.7	2.0
Control	2.2±0.6	0.9±0.2	2.0